Advanced and Sustainable Technologies (ASET) eISSN 2976-2294
Volume 2, No 1, June 2023 [38-47]

Response Surface Optimisation of the Mechanical Shock Testing for Advanced Ball Grid Array Package

Muhammad Syahmi Ahmad Tamili[1*]

[1]Faculty of Mechanical Engineering & Technology, Universiti Malaysia Perlis, Perlis, Malaysia.

Received 27 March 2023, Revised 18 May 2023, Accepted 20 May 2023

ABSTRACT

This research focuses on optimising mechanical shock testing for advanced ball grid array (BGA) packages using finite element analysis. This research aims to analyse the parameters in mechanical shock testing for advanced BGA packages and optimise their mechanical strength using Response Surface Methodology (RSM). This research employs two methods: Finite Element Analysis and RSM. The methodology involves investigating three parameters: impact frequency, stand-off height, and solder ball diameter through numerical experimentation. Three responses, namely stress, strain, and displacement, are obtained to achieve an optimal result using RSM. The numerical experiments are conducted using finite element software, specifically on advanced BGA packages. The findings of this study contribute to result optimisation and provide an understanding of the most significant parameters and responses. High displacement affects neighbouring circuit board parts and solder joints, leading to broken links and connections. Besides, high acceleration could lead to loose bolts, relay chattering, and slipping of the variable resistor in integrated circuit (IC) packages. The validation process is performed to verify the results obtained from the numerical experiments.

Keywords: Ball Grid Array (BGA), Response Surface Methodology, Mechanical shock test, Finite element analysis

1. INTRODUCTION

Electronic devices are susceptible to shock and vibration during transportation and accidental drops, which can lead to the failure of delicate electronic interconnects [1]. Mechanical shock testing is a commonly employed method for evaluating the robustness of electronic components [2]. It involves subjecting the test specimen to sudden and intense forces to assess its performance under such conditions. Traditional research methods rely on monitoring electrical resistance to detect impending failures. However, this approach only provides information about failures after they occur, limiting its effectiveness for applications that require early detection. The simulation method [3] can quantify failures in electronic assemblies exposed to shock and vibration without relying on electrical resistance testing. Besides, it also provides an understanding of the effects of shock and vibration on electronic assemblies [4] and identifies potential failure mechanisms before they manifest as electrical issues.

Liu et al. conducted a study to explore three accelerated test methods for evaluating the mechanical reliability of printed circuit boards (PCBs) at the board level using vibration loadings [5]. The first method employed fixed-frequency sine vibration, while the second method utilised swept sine vibration within a limited frequency range. The third method involved sweeping random vibration within a specific frequency band. To capture the response of the PCBs, a high-speed strain data acquisition system was employed, and the frequency characteristics were determined through Fast Fourier Transform (FFT) analysis of the strain data collected during the

*Corresponding author: syahmi300594@gmail.com

vibration tests. Vibration failure testing is crucial in understanding the degradation process and failure mechanisms of solder joints in electronic packaging [6]. The vibration environment of jet aircraft instrumentation equipment serves as a reference to determine the applied vibration load. The voltage amplitude of the solder joints is varied from 0 to 5V, representing the transition from the initial state to eventual failure. The study incorporates environmental tests, and devises solder joint health monitoring circuits to facilitate the investigation. Solder joints in electronic packaging are essential for mechanical fixation and electrical interconnection between electronic chips and printed circuit boards. This work [6] focused on characterising solder joint health and developing degradation models under vibration loads.

Traditional reliability assessments of electronic devices have focused on developing structural integrity models to predict their operational lifespan in vibratory and thermal environments [7]. While extensive research has been carried out on the thermal characteristics of solder joints [8], the impact of dynamic loading [9] on solder joint fatigue life has received limited attention. The underlying material science governing solder joint failure under vibration remains partially understood. In a study conducted by Basaran et al. (2002) [10], a comprehensive test program was implemented to investigate the inelastic behaviour of solder joints within ball grid array (BGA) packages. The findings uncovered that when subjected to elevated temperatures, vibration and shock can lead to the accumulation of inelastic strains and damage in solder joints. Contrary to the prevailing belief that all strains induced by vibration are purely elastic, this study demonstrates that vibration can induce significant inelastic strains.

In analysing mechanical shock testing on advanced Ball Grid Array (BGA) packages, the Finite Element Method (FEM) proves to be a suitable approach [11]. FEM is a computational technique used to solve complex problems in engineering and design by dividing them into smaller, more manageable elements [12]. Unlike analytical methods, FEM allows for analysing real-world, intricate problems that cannot be easily solved using conventional approaches. For instance, while the classical theory of materials or elasticity theory can provide approximate stress and strain calculations for a simple beam, they would not be efficient in understanding the behaviour of a component within a complex system like an automotive suspension during cornering. The application of FEM extends beyond mechanical shock testing. It encompasses various engineering disciplines, including structural analysis [13], solid mechanics [14], dynamics [15], thermal analysis [16], electrical analysis [17], and biomaterials [18].

In this project, FEM is utilised to investigate the displacement, stress, and strain experienced by the BGA during mechanical shock testing. The use of FEM in testing is crucial as it allows for obtaining results through simulation, reducing the need for costly and time-consuming physical testing. Response surface methodology is applied in the design of numerical experiments and optimised the mechanical responses. The outcomes of this study hold significant benefits for researchers and professionals in the electronic component industry. The analysis conducted in this numerical experiment contributes to improving the quality and reliability of Printed Circuit Boards (PCBs) by examining the mechanical strength of BGAs. This information will also be valuable for users of electronic components, as they can gain insights into the mechanical behaviour of BGAs and make informed decisions to avoid potential failures when using these components in their applications.

2. MATERIAL AND METHODS

This research aimed to optimise the mechanical shock testing of advanced ball grid array (BGA) packages using a response surface approach and finite element analysis. The Response Surface Methodology (RSM) was employed to optimise the numerical parameters involved in the testing. The BGA packages' stress, strain, and displacement were analysed through finite element analysis. Design Expert software was utilised to perform the Design of Experiment (DOE) to facilitate the

numerical experimentation. This aided in determining the appropriate experimental conditions and parameter settings. Besides, Solidworks software was employed to design the 3D advanced BGA packages. The designed BGA package model was then exported to finite element software for conducting simulation tests using the optimised numerical parameters. Using numerical simulations and design optimisation techniques enables researchers to enhance the reliability and performance of BGA packages, ultimately leading to improved electronic component designs.

The BGA assembly was meticulously designed using Solidworks software, providing a detailed and comprehensive 3-dimensional view of the assembly. The designed model, created using various tools in Solidworks, such as circles, lines, extrusions, and fillets, was then imported into finite element software to conduct the simulation. The isometric view of the BGA assembly can be observed in Figure 1, showcasing the intricate details and geometry of the design.

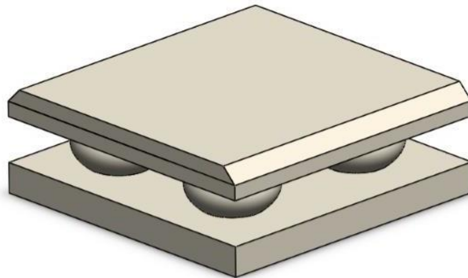

Figure 1: Isometric view of BGA assembly.

The dimensions of the BGA are 15 mm × 15 mm in length and width. These dimensions were determined based on the design requirements. As shown in Table 1, the numerical experiment involved fixed variables, including package length, package width, substrate thickness, and silicon chip thickness. These variables were carefully chosen to investigate their impact on the mechanical characteristics of the BGA packages during the experiment. Tables 2 and 3 summarise the range value of the factor and the mechanical properties used in the finite element analysis.

Table 1: The variable value used in 3D BGA.

Variable	Value
Package length, mm	15
Package width, mm	15
Substrate thickness, mm	0.4
Silicon chip thickness, mm	0.9

Table 2: The range value of the factor.

Factor	Range value
Frequency, f (Hz)	$50 < f < 100$
Stand-off height, h (mm)	$0.3 < h < 0.5$
Solder ball diameter, d (mm)	$0.4 < d < 0.6$

Table 3: Density, Young's modulus and Poisson's ratio [19].

Part	Density, ρ, Kg/m3	Young's Modulus, E (GPa)	Poisson's ratio, v
Solder ball	1035	32	0.4
Substrate	9000	16	0.3
Silicon chip	8410	160	0.3
PCB	2680	17	0.3

2.1 Design of Experiment

Response Surface Methodology (RSM) was employed to analyse the variable research data and responses for optimal results. Design Expert software was utilised to facilitate the data collection and generate a Central Composite Design (CCD) table. As shown in Table 4, the table presents the levels of the designing parameters considered in this study. Each factor in the research was represented by three different levels: high level (+1), medium level (0), and low level (-1). Twenty numerical experiments were conducted using the Central Composite Design (CCD) layout to obtain the optimum result. Each experiment was run with a specific combination of factor levels. The formation of these twenty simulation runs was determined according to Equation 1.

$$CCD = 2^k + 2k + 6 \quad (1)$$

where k represents as number of factors involved.

Table 4: Level of designing parameter.

No	Factor	Unit	Level		
			Low (-1)	Medium 0	High (+1)
1	Frequency, f	Hz	50	75	100
2	Stand-off height, h	mm	0.3	0.4	0.5
3	Solder ball diameter, d	mm	0.4	0.5	0.6

3. RESULTS AND DISCUSSION

3.1 Result of Central Composite Design (CCD)

The simulation experiment has been conducted. A total of twenty times in accordance with the Central Composite Design (CCD) equation, which is $CCD = 2^k+2k+6$, where k represents the number of factors involved. As indicated in Table 5, different data values (-1, 0, and 1) were prepared for each factor to generate the response values in this experiment. The responses were obtained from the twenty simulation runs, each utilising different factor data values. Table 5 summarises the coding of the factor values and responses. Factor A represents the Frequency, Factor B represents the stand-off height, and Factor C represents the solder ball diameter. The data generated using the CCD concept was employed in this study. The primary objective of the experiment was to determine the optimum response values for mechanical shock applied to the BGA. The maximum response value from each run was selected and recorded in the CCD table, as presented in Table 5.

The simulation generated response results such as stress, strain, and frequency. The values of frequency, solder ball diameter, and stand-off height were inserted into the finite element software to run the simulation on the BGA model. These values were obtained from the CCD table. In Figure 2, the colour distribution represents the distribution of responses on the BGA after implementing the simulation in run 20. The redder colour indicates areas of maximum stress within the BGA, while the bluer colour represents areas with minimum stress. Selecting the maximum response results from the simulation and inserting them into the CCD table is to determine the optimal outcome, as the maximum values are crucial in achieving this objective.

Table 5: Result of central composite design (CCD).

	Factor (Coded)			Response		
Run	A	B	C	Stress (GPa)	Displacement (mm)	Strain (10^{-3})
1	-1	-1	-1	7.855358	1.18852	241.575
2	1	-1	-1	7.389518	1.38933	228.719
3	-1	1	-1	3.616248	1.24660	113.054
4	1	1	.J	3.61624	1.24660	113.054
5	-1	-1	1	12.8792	1.25457	299.323
6	1	-1	1	12.8792	1.25450	299.323
7	-1	1	1	31.1847	1.08815	162.287
8	1	1	1	48.1316	1.13754	331.345
9	-1	0	0	43.0205	1.28755	279.379
10	1	0	0	54.0332	1.15204	330.908
11	0	-1	0	7.90302	1.18991	200.904
12	0	1	0	40.8713	1.32017	272.997
13	0	0	-1	6.18876	1.25239	193.940
14	0	0	1	8.79333	1.29464	257.243
15	0	0	0	43.0205	1.28755	279.379
16	0	0	0	43.0205	1.28755	279.379
17	0	0	0	43.0205	1.28755	279.379
18	0	0	0	43.0205	1.28755	279.379
19	0	0	0	43.0205	1.28755	279.379
20	0	0	0	43.0205	1.28755	279.379

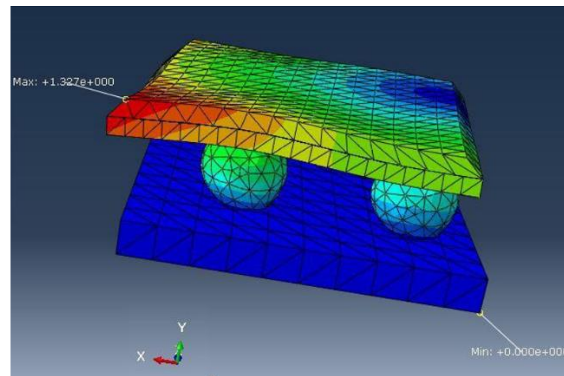

Figure 2: Displacement contour of BGA assembly.

3.2 Effect of Factors on the Response

The effects of frequency, stand-off height, and solder ball diameter on the responses were evaluated using perturbation graphs, as depicted in Figures 3-5. Each perturbation graph displayed the plot of factors A, B, and C, where A represents frequency, B represents stand-off height, and C represents solder ball diameter. These graphs were used to identify the relationship between the factors and the responses. They also revealed the correlations among frequency, stand-off height, and solder ball diameter and the way they affected the responses. A quadratic behaviour is observed in Figure 3, which represents the perturbation graph for response 1 (stress). Based on the graph, it can be seen that the factors that have a more significant influence on stress are frequency (A) and solder ball diameter (C). The perturbation graph shown in Figure 3 demonstrates this quadratic relationship. Figure 4 depicts the perturbation graphs for response 2, which represents displacement. Unlike the previous perturbation graph, Figure 4 exhibits a linear behaviour. In this perturbation plot, the displacement shows the linear correlation to the factors A, B and C. As the graph indicates, the factors that significantly affect displacement are

frequency (A) and solder ball diameter (C). In Figure 5, the perturbation plots for response 3 (strain) demonstrate that the most significant factors are frequency (A) and solder ball diameter (C). The graph exhibits a quadratic behaviour, indicating a more complex relationship between these factors and the strain response.

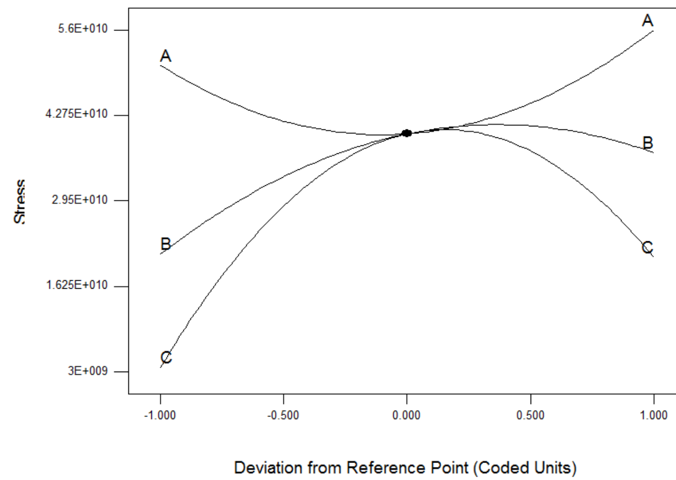

Figure 3: The perturbation graph for response 1 stress.
(Note A= frequency, B=standoff height, C= solder ball diameter)

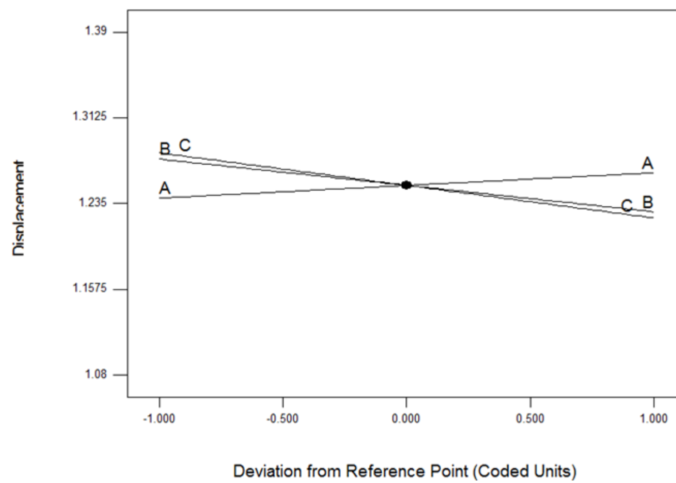

Figure 4: The perturbation graph for response 2, displacement.
(Note A= frequency, B= standoff height, C= solder ball diameter)

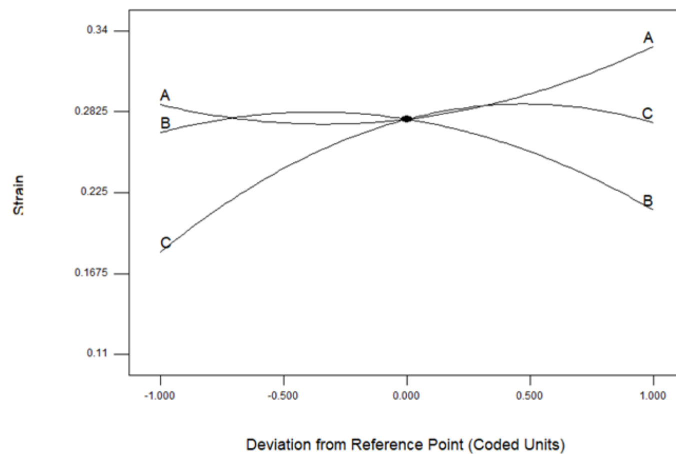

Figure 5: The perturbation graph for response 3, strain.
(Note A= frequency, B=standoff height, C= solder ball diameter)

The correlation between factors and responses was further examined using 3D surface graphs generated by Design Expert, as depicted in Figures 6-8. These graphs illustrate the relationship between each factor and its corresponding response. The significant factors were selected for the 3D surface graphs, showcasing the distribution of factor levels and their impact on each response. In Figure 6, the 3D surface graph displays the stress response. The redder regions indicate the maximum stress values, while the bluer regions represent the minimum stress values. For instance, the maximum stress value is 5.4×10^{10} Pa, achieved at a frequency of 100 Hz and a solder ball diameter of 0.5 mm (Run 10). On the other hand, the minimum stress value is 3.62×10^{9} Pa, attained at a frequency of 75 Hz and a solder ball diameter of 0.4 mm (Run 13). Notably, the factors of frequency and solder ball diameter were selected due to their significant influence on the stress response.

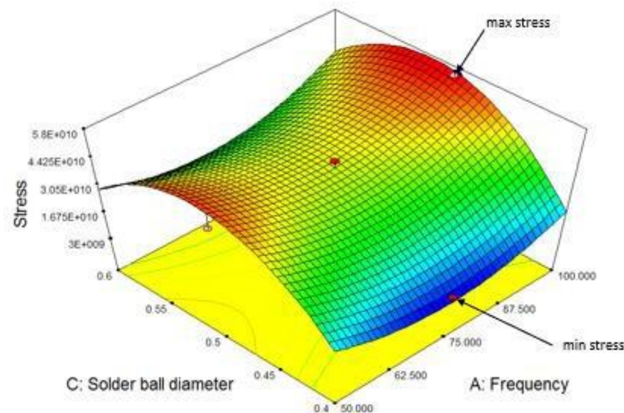

Figure 6: 3D surface graph for response 1, stress.

In Figure 7, the 3D surface graph represents the displacement. The graph shows the distribution of colour, indicating different levels of displacement based on the selected factors. The frequency and solder ball diameter factors were chosen as they significantly influence the displacement response, as depicted in Figure 7. The maximum displacement value is 1.39 mm, achieved at a frequency of 75.00 Hz and a stand-off height of 0.5 mm (Run 12). Conversely, the minimum displacement value is 1.09 mm, obtained at a frequency of 100 Hz and a stand-off height of 0.4 mm (Run 10).

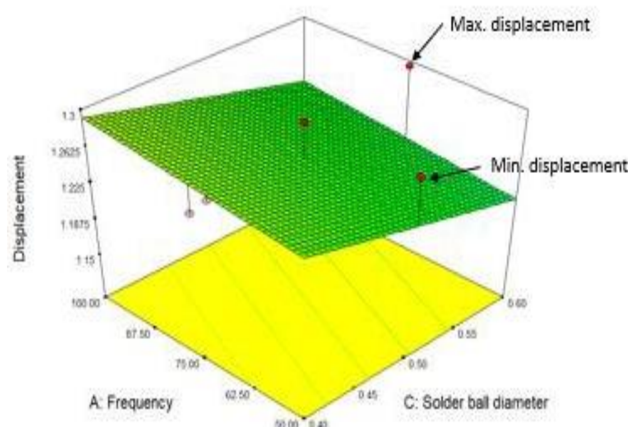

Figure 7: 3D surface graph for response 2, displacement.

Figure 8 illustrates the 3D surface graph depicting the distribution of colour representing different strain levels. The graph shows the maximum and minimum strain values achieved under varying conditions. The maximum strain value recorded is 0.33, obtained at a frequency of 100.00 Hz and a stand-off height of 0.40 mm. This maximum strain value corresponds to a standard order

of 10 in the CCD table. On the other hand, the minimum strain value observed is 0.11, achieved at a frequency of 75.00 Hz and a stand-off height of 0.30 mm, with a standard order of 11 in the CCD table. Figure 8 provides valuable insights into the relationship between the selected factors (frequency and stand-off height) and the resulting strain. The graph enables the visualisation of how different combinations of these factors impact the strain response.

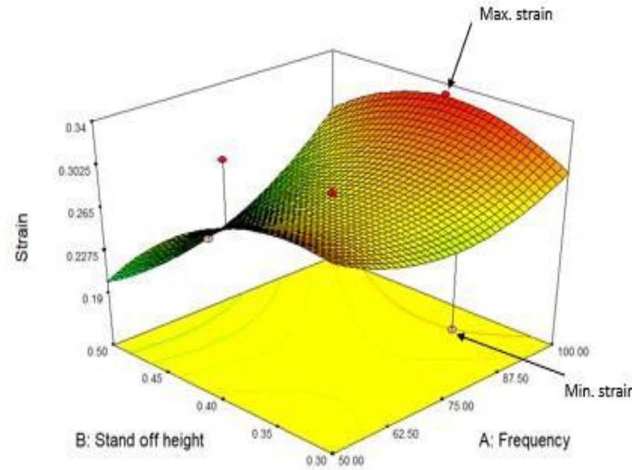

Figure 8: 3D surface graph for response 3, strain.

3.3 Optimisation of Design Parameters

The objective of optimisation was to maximise the stress, displacement, and strain responses based on the recommendations provided by the Design Expert software. Optimisation played a crucial role in this experiment as it aimed to achieve the optimum results for the factors under investigation. Table 6 compares the optimal values recommended by the Design Expert software and the actual values of the responses obtained from simulating finite element software using the recommended optimal factor values. This comparison allows for an evaluation of how closely the actual responses align with the optimised values suggested by the software.

Table 6: The optimum value for the factor and the responses as recommended by Design Expert software and the simulation result.

	Frequency	Stand-off height	Solder ball diameter	Stress, Pa	Displacement, mm	Strain
Design Expert	50.00	0.50	0.40	3.61×10^9	1.25	0.11
Simulation	50.00	0.50	0.40	3.62×10^9	1.25	0.11

3.4 Validation of Simulation Results

After obtaining the optimal values through the optimisation process using Design Expert and Response Surface Methodology (RSM), a validation process was conducted to ensure the numerical experiment's success. The optimal values were validated using finite element software. Based on Table 6, the optimal values for the frequency, stand-off height, and solder ball diameter were determined to be 50 Hz, 50 mm, and 0.4 mm, respectively. The corresponding optimal values for the responses were 3.61×10^9 Pa for stress, 1.25 mm for displacement, and 0.11 for strain. To validate the results, the percentage difference was calculated. The percentage error does not exceed 10% [20] was used in previous work. The percentage error for frequency was 0.28%, indicating a minimal deviation from the optimal value. The displacement and strain had exact values that matched the optimal values precisely. This validation process ensures the reliability of the optimised results. It confirms that the numerical experiment successfully achieved the desired outcomes within an acceptable margin of error.

4. CONCLUSION

In this experiment, the Response Surface Methodology (RSM) was used to optimise the design parameters and investigate the correlation between the parameters and responses. The design parameters included frequency, stand-off height, and solder ball diameter, while the responses were stress, displacement, and strain. The analysis revealed that frequency and solder ball diameter were the most significant factors influencing the responses. The simulation was conducted 20 times using the Central Composite Design (CCD) equation. The Design Expert software was utilised to optimise the data and provide suggested optimal values for the parameters and responses. The comparison between the suggested values from Design Expert and the results obtained from the simulation indicated a successful optimisation process. The suggested parameter values fell within the initial experiment's set range, while the suggested response values closely matched the actual values obtained from simulations. The optimal values suggested by Design Expert were 50.04 Hz for frequency, 0.50 mm for stand-off height, and 0.40 for solder ball diameter. The suggested response values were 3.61×10^9 Pa for stress, 1.25 mm for displacement, and 0.11 for strain. The validation process was conducted using the percentage difference to ensure the reliability of the results. Successful validation confirmed the accuracy of the experiment's outcomes. Overall, the optimisation and validation processes effectively determined optimal parameter values and validated the results, thus demonstrating the study's success.

ACKNOWLEDGEMENTS

The author would like to express sincere gratitude to the staff of the Faculty of Mechanical Engineering & Technology, Universiti Malaysia Perlis (UniMAP), for their valuable technical support throughout the study.

REFERENCES

[1] Ledezma-Ramírez, D. F., Tapia-González, P. E., Ferguson, N., Brennan, M., & Tang, B. Recent advances in shock vibration isolation: An overview and future possibilities. Applied Mechanics Reviews, vol 71, issue 6 (2019).

[2] Sood, B., Das, D., & Pecht, M. Screening for counterfeit electronic parts. Journal of Materials Science: Materials in Electronics, vol 22, (2011) pp. 1511-1522.

[3] Alsaleem, F. M., Younis, M. I., & Ibrahim, M. I. A study for the effect of the PCB motion on the dynamics of MEMS devices under mechanical shock. Journal of Microelectromechanical Systems, vol 18, issue 3 (2009) pp.597-609.

[4] García-Pérez, A., Sorribes-Palmer, F., Alonso, G., & Ravanbakhsh, A. FEM simulation of space instruments subjected to shock tests by mechanical impact. International Journal of Impact Engineering, vol 126, (2019) pp. 11-26.

[5] Liu, Y., Sun, F. L., Zhang, H. W., Wang, J., & Zhou, Z. Evaluating board level solder interconnects reliability using vibration test methods. Microelectronics Reliability, vol 54, issue 9-10 (2014) pp. 2053-2057.

[6] Sheng, Z., Jing, B., Tang, W., Hu, J., & Dong, J. Effects of different vibration directions on the damage mechanism of BGA under vibration loading coupled with cyclic thermal. In 2016 Prognostics and System Health Management Conference (PHM-Chengdu), (2016) pp. 1-5.

[7] Jiang, N., Zhang, L., Liu, Z. Q., Sun, L., Long, W. M., He, P., ... & Zhao, M. Reliability issues of lead-free solder joints in electronic devices. Science and technology of advanced materials, vol 20, issue 1 (2019) pp. 876-901.

[8] Depiver, J. A., Mallik, S., & Harmanto, D. Solder joint failures under thermo-mechanical loading conditions–A review. Advances in Materials and Processing Technologies, vol 7, issue 1 (2021) pp. 1-26.

[9] Salameh, A. A., Hosseinalibeiki, H., & Sajjadifar, S. Application of deep neural network in fatigue lifetime estimation of solder joint in electronic devices under vibration loading. Welding in the World, vol 66, issue 10 (2022) pp. 2029-2040.

[10] Basaran, C., Tang, H., & Nie, S. Experimental damage mechanics of microelectronic solder joints under fatigue loading. In ASME International Mechanical Engineering Congress and Exposition, vol 36401, (2002) pp. 229-236.

[11] Wong, S. F., Malatkar, P., Rick, C., Kulkarni, V., & Chin, I. Vibration testing and analysis of ball grid array package solder joints. In 2007 Proceedings 57th Electronic Components and Technology Conference, (2007) pp. 373-380.

[12] Okereke, M., & Keates, S. Finite element applications. Cham: Springer International Publishing AG, Springer, (2018).

[13] Chethan, K. N., Zuber, M., Shenoy, S., & Kini, C. R. Static structural analysis of different stem designs used in total hip arthroplasty using finite element method. Heliyon, vol 5, issue 6 (2019) p. e01767.

[14] Cardiff, P., & Demirdžić, I. Thirty years of the finite volume method for solid mechanics. Archives of Computational Methods in Engineering, vol 28, issue 5 (2021) pp. 3721-3780.

[15] Costa, J. N., Antunes, P., Magalhães, H., Pombo, J., & Ambrósio, J. A finite element methodology to model flexible tracks with arbitrary geometry for railway dynamics applications. Computers & Structures, vol 254, (2021) p. 106519.

[16] Carlini, M., McCormack, S. J., Castellucci, S., Ortega, A., Rotondo, M., & Mennuni, A. Modelling and numerical simulation for an innovative compound solar concentrator: Thermal analysis by FEM approach. Energies, vol 13, issue 3 (2020) p. 548.

[17] Saturnino, G. B., Madsen, K. H., & Thielscher, A. Electric field simulations for transcranial brain stimulation using FEM: an efficient implementation and error analysis. Journal of neural engineering, vol 16, issue 6 (2019) p. 066032.

[18] Wadatkar, N. D., Londhe, S. D., & Metkar, R. M. Stress Analysis of Fractured Femur Bone and Implant of Different Metallic Biomaterials. Trends in Biomaterials and Artificial Organs, vol 34, issue 3 (2020) pp. 96-100.

[19] Chen, Y. S., Wang, C. S., & Yang, Y. J. Combining vibration test with finite element analysis for the fatigue life estimation of PBGA components. Microelectronics Reliability, vol 48, issue 4 (2008) pp. 638-644.

[20] Lim, W. T., Ooi, E. H., Foo, J. J., Ng, K. H., Wong, J. H., & Leong, S. S. The role of shear viscosity as a biomarker for improving chronic kidney disease detection using shear wave elastography: A computational study using a validated finite element model. Ultrasonics, (2023) p. 107046.